CHEMISTRY
A EUROPEAN JOURNAL

DOI: 10.1002/chem.201102195

Molecular Interactions between Glycopeptide Vancomycin and Bacterial Cell Wall Peptide Analogues

Bengang Xing,* Tingting Jiang, Xiangyang Wu, Roushen Liew, Jie Zhou, Dawei Zhang,* and Edwin K. L. Yeow*[a]

Abstract: The molecular interactions of the glycopeptide antibiotic vancomycin (Van) with bacterial cell wall analogues *N*,*N*′-diacetyl-L-Lys-D-Ala-D-Ala (Ac_2KDADA) and *N*,*N*′-diacetyl-L-Lys-D-Ala-D-Lac (Ac_2KDADL) were investigated in neat water, phosphate buffer and HEPES buffer by using fluorescence correlation spectroscopy (FCS) and molecular dynamics (MD) simulations. The FCS determined dissociation constants (k_d) show that the intrinsic binding affinity between Van and the drug-sensitive peptide ligand Ac_2KDADA remains invariant when the solvent is changed from neat water to either PBS or HEPES buffer; this demonstrates that there are no obvious solvent effects on the association between Van and Ac_2KDADA due to the strong intermolecular interaction between the two moieties. When compared to Ac_2KDADA, a significantly larger k_d value was observed for the binding between the drug-resistant peptide ligand Ac_2KDADL and Van. Furthermore, the k_d increased by about 8- to 11-times when the solvent was changed from neat water to 10 mM phosphate/HEPES buffer. The stability of the Ac_2KDADL–Van complex was dependent on the concentration of the buffer and k_d increases as the concentration of either phosphate ions or HEPES increased until an equilibrium was attained. Both FCS and MD simulation studies clearly showed that the components constituting the buffer solution (e.g., phosphate ions and HEPES) are involved in molecular interactions with the binding pocket of Van and they profoundly affect the intrinsic stability of the complex formed between the low-affinity Ac_2KDADL and Van. These results could help us to better understand the detailed structure and activity of glycopeptide antibiotic derivatives toward bacterial cell wall peptide analogues, and can further facilitate the development of new drug candidates against drug-resistant bacterial strains.

Keywords: antibiotics · buffers · drug interactions · fluorescence correlation spectroscopy · molecular dynamics

Introduction

The glycopeptide antibiotic vancomycin (Van) is often used as a last resort to effectively treat methicillin resistant *Staphylococcus aureus* (MRSA).[1] The mode of action of Van involves the selective binding of the antibiotic to the -D-Ala-D-Ala termini of the bacteria cell wall peptidoglycan; this leads to an inhibition of cell growth and eventual cell death. With the frequent use of this antibiotic molecule, some drug resistant Gram positive bacterial pathogens, such as vancomycin-resistant *enterococci* (VRE), have emerged, which are capable of assembling the peptidoglycan precursors and switching the termini -D-Ala-D-Ala to -D-Ala-D-Lac.[2] This undesired microbial development results in a drastic drop in the binding affinity between Van and the resistant bacteria and renders the drug ineffective in the fight against VRE-related infections, which have now become a major and worldwide public health threat. There is, therefore, a new urgency to understand the detailed structure and activity of vancomycin antibiotic derivatives with the aim of developing new drug candidates against evolving bacterial pathogens.[2]

In order to design Van derivatives that exhibit improved antimicrobial activity against both Van-receptive and Van-resistant bacteria, it is necessary to understand the driving force behind the interaction between the antibiotic and bacteria cell wall mimicking peptide ligands. The binding affinities between Van and the ligands *N*,*N*′-diacetyl-L-Lys-D-Ala-D-Ala (Ac_2KDADA) and *N*,*N*′-diacetyl-L-Lys-D-Ala-D-Lac (Ac_2KDADL) in buffer solutions have been previously investigated by using several methods including UV-difference spectroscopy,[3,4] fluorescence,[5–7] affinity capillary electrophoresis,[8] isothermal titration microcalorimetry,[9] and NMR spectroscopy.[10] The association between Van and cell wall analogues has also been studied in the gas-phase by using mass spectrometry.[11] There exists a discrepancy between the various reported binding constant values, which

[a] Prof. Dr. B. G. Xing, T. Jiang, Dr. X. Wu, R. Liew, J. Zhou, Prof. Dr. D. Zhang, Prof. Dr. E. K. L. Yeow
Division of Chemistry and Biological Chemistry
School of Physical and Mathematical Sciences
Nanyang Technological University
Singapore 637371 (Singapore)
Fax: (+65) 6791-1961
E-mail: edwinyeow@ntu.edu.sg
Zhangdw@ntu.edu.sg
Bengang@ntu.edu.sg

Supporting information for this article is available on the WWW under http://dx.doi.org/10.1002/chem.201102195.

has been ascribed to the different experimental techniques and analysis methods used.[13,14] The degree of association between Van and Ac_2KDADA has also been shown to be affected by solvent properties, such as pH, ionic strength and the type of solvents used; this indicates, in general, the complexity of the intermolecular interaction.[6,12] Despite extensive studies on the environmental effects on the binding between Van derivatives and bacterial cell wall peptide precursors, the exact nature of the inconsistency in the equilibrium binding constant values reported so far remains vague.[13,14] In buffer solutions, detailed information on the effects of the various components that make up the buffer (e.g., phosphate ion in phosphate buffer, etc.) on the association between Van and peptide analogues need to be further explored since buffer solutions are known to interfere with the coupling between ligands and biological receptors and their effects should therefore be carefully characterized.[15,16]

In this study, single-molecule fluorescence correlation spectroscopy (FCS) was used, for the first time, to investigate the association between Van and cell wall analogues terminating in -D-Ala-D-Ala and -D-Ala-D-Lac in the commonly employed vancomycin and bacterial cell wall peptide precursor interaction buffer systems: phosphate and HEPES buffers. FCS is based on the analysis of the diffusion of an emitting molecule as it diffuses in the excitation volume of a confocal microscope (Scheme 1). The difference in diffusion

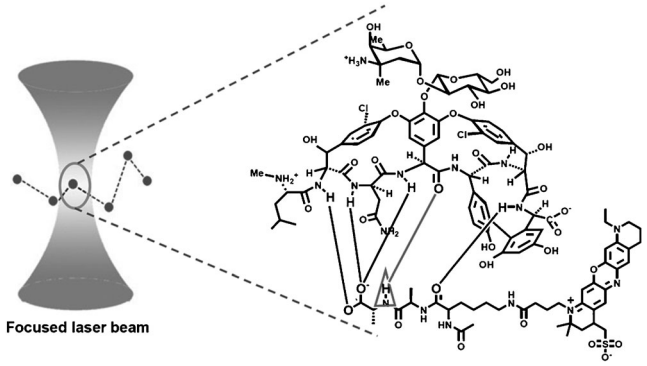

Scheme 1. Schematic representation of the FCS study of the molecular interaction between Van and dye-labeled bacterial cell wall peptide analogues. A single complex formed by the association of the two moieties diffuses across the ellipsoidal excitation/observation volume.

behavior between a freely diffusing emitting molecule and when it binds to a target allows the quantification of the corresponding binding constant between the two species. FCS is now recognized to be a very simple yet powerful technique for studying ligand–receptor interaction in biomolecular recognition.[17] Unlike UV-difference spectroscopy and conventional fluorescence techniques, one major advantage of FCS is that it does not require the utilization of an environment-sensitive chromophore that alters its photophysical properties (e.g., emission quantum yield, absorption coefficient) upon complex formation between the labeled ligand and substrate. In addition, FCS requires relatively low concentrations of peptide and Van and hence avoids complications arising from peptide aggregation and Van dimerization, which commonly occur when high concentrations of peptide/antibiotics are used.[8] Herein, the peptide sequences Ac_2KDADA and Ac_2KDADL were labeled with ATTO 655, which is a photostable and commonly used near-infrared fluorescent (NIR) dye in FCS studies.[18] The molecular interaction between the fluorescent labeled/nonlabeled peptide sequences and Van and the influence of phosphate and HEPES buffers on the intrinsic binding between the two moieties were systematically investigated by using both single-molecule FCS and molecular dynamics (MD) simulations.

Results and Discussion

The peptide precursors were first modified by ATTO 655 NHS and further purified by RP-HPLC (see the Experimental Section for details). Figure 1 shows the normalized auto-

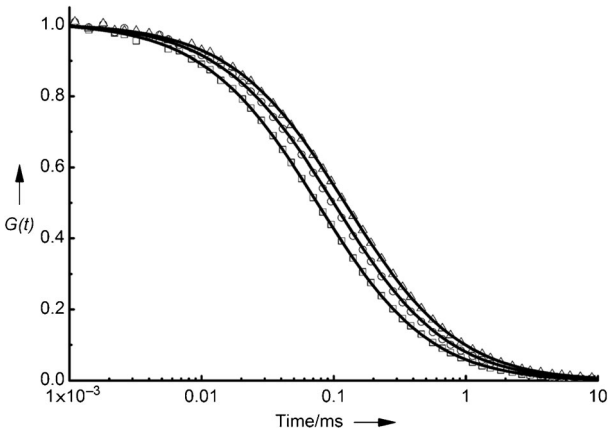

Figure 1. Nomalized autocorrelation functions of ATTO 655 dye (□), Ac(ATTO 655)KDADA (○) and Ac(ATTO 655)KDADA in the presence of Van (50 μM) (△) in neat water.

correlation functions of freely diffusing ATTO 655 dye, labeled Ac(ATTO 655)KDADA peptide and Ac-(ATTO 655)KDADA in the presence of Van (50 μM) in neat water. Since the triplet state formation quantum yield of ATTO 655 is negligible, the FCS autocorrelation function of Ac(ATTO 655)KDADA is well-fitted to Equation (1):[18]

$$G(t) = G_0\left(1 + \frac{t}{\tau}\right)^{-1}\left(1 + \frac{t}{\kappa^2\tau}\right)^{-\frac{1}{2}} \quad (1)$$

where τ (=98.8 μs) is the diffusion time and κ is the eccentricity of the confocal volume defined by $\kappa = z_0/\omega_0$ (ω_0 and z_0 are the lateral radius and axial $1/e^2$ radius of the confocal volume, respectively). The diffusion coefficient for Ac-

(ATTO 655)KDADA in neat water is obtained from Equation (2):

$$\tau = \frac{\omega_0^2}{4D} \tag{2}$$

which yields $D = 310(\pm 2)\ \mu m^2 s^{-1}$. At high Van concentrations (i.e., 50 μM) the autocorrelation function is best described by using Equation (1) with $\tau = 128$ μs. This suggests an insignificant amount of free labeled peptide ligand present in the Van (50 μM) solution and the diffusion time is ascribed to the diffusion of Ac(ATTO 655)KDADA–Van complex across the observed volume. A value of $D = 240(\pm 2)\ \mu m^2 s^{-1}$ is calculated for the bound complex with Equation (2). As expected, in the presence of Van, the labeled peptide ligand bound to Van diffuses more slowly across the observed volume. It is worth noting that the diffusion coefficient of ATTO 655 remains invariant in the different solvents used in this study, indicating the insignificant effect of viscosity. In addition, the change in emission quantum yield when the labeled peptide ligand is bound to the antibiotic is small (<10%) and was not considered in further analysis.[19]

The binding equilibrium between Van (V) and Ac(ATTO 655)KDADA (L) is described by the reaction L+V⇄LV, where LV is the Ac(ATTO 655)KDADA–Van complex and the corresponding association constant (k_{a1}) and dissociation constant (k_{d1}) are related by Equation (3):

$$k_{a1} = \frac{1}{k_{d1}} = \frac{[LV]}{[L][V]} \tag{3}$$

When an intermediate concentration of Van is incubated with Ac(ATTO 655)KDADA, the autocorrelation function of the sample solution measured is best fitted to a two-component model that takes into account the diffusion times of both the free labeled peptide ligand (τ_L) and the labeled bound complex (τ_{LV}):

$$G(t) = N^{-1}\left[(1 - Y)\left(1 + \frac{t}{\tau_L}\right)^{-1}\left(1 + \frac{t}{\kappa^2 \tau_L}\right)^{-\frac{1}{2}} + Y\left(1 + \frac{t}{\tau_{LV}}\right)^{-1}\left(1 + \frac{t}{\kappa^2 \tau_{LV}}\right)^{-\frac{1}{2}}\right]$$

with the relative proportion of LV given by Equation (4):

$$Y = \frac{[LV]}{[L] + [LV]} \tag{4}$$

The dissociation constant, k_{d1}, is obtained by fitting the graph of Y against [V] by using the following equation:[19]

$$Y = [L]_0^{-1}\left[\left(\frac{k_{d1} + [L]_0 + [V]_0}{2}\right) - \sqrt{\left(\frac{k_{d1} + [L]_0 + [V]_0}{2}\right)^2 - [L]_0[V]_0}\right]$$

where $[L]_0$ and $[V]_0$ are the initial concentrations of L and V, respectively. Figure 2 shows the graph of Y against various concentrations of Van, [V], and clearly indicates an increase in binding upon increasing [V]. Based on this fluorescence binding assay, a dissociation constant of $k_d = 1.1(\pm 0.1)$ μM was obtained for Ac(ATTO 655)KDADA in neat water.

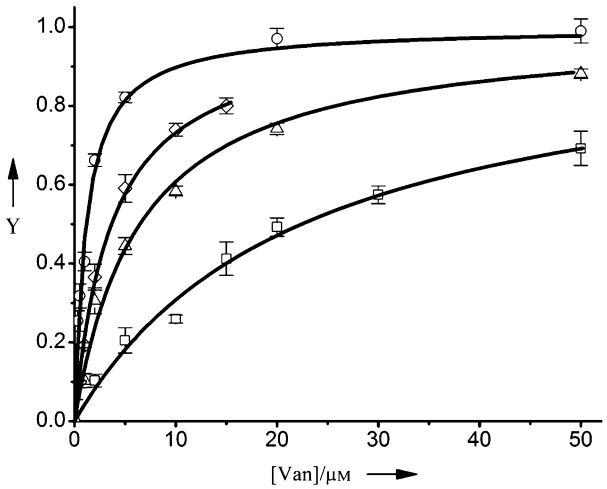

Figure 2. Plots of Y versus [Van] for Ac(ATTO 655)KDADA in neat water (○) and Ac(ATTO 655)KDADA in the presence of Ac_2KDADL (5 mM) in neat water (□), 5 mM phosphate buffer (△) and 10 mM phosphate buffer (◇).

The binding constant of labeled Ac(ATTO 655)KDADL to Van cannot be directly determined by using FCS since the autocorrelation function in neat water does not vary significantly when Van is added into the solution. This demonstrates that the binding between Van and the low-affinity ligand is negligible for the concentrations of peptide (1.5 nM) and Van (between 0 and 50 μM) used in the FCS experiment. Larger amounts of Van are avoided due to possible dimerization of the antibiotics at high concentrations.[8] In order to precisely investigate the weak Van-binding affinity of the peptide with D-Ala-D-Lac, an FCS-based competitive binding assay was used in which the non-labeled Ac_2KDADL ligand competed with Ac(ATTO 655)KDADA for binding to Van. In this case, Van was added to a mixture containing Ac(ATTO 655)KDADA (1.5 nM) and Ac_2KDADL (I; 5 mM). The association constant for the formation of Ac(ATTO 655)KDADA–Van complex is given by Equation (3), while the association (k_{a2}) and dissociation (k_{d2}) constants for binding between Van (V) and I (i.e., I+V⇄IV) are given by Equation (5):

$$k_{a2} = \frac{1}{k_{d2}} = \frac{[IV]}{[I][V]} \tag{5}$$

The relationship between the initial concentration of Van ($[V]_0$) and the binding proportion (Y) of Ac(ATTO 655)KDADA to Van, in competition with the unlabeled peptide I, is expressed as:[20]

$$[V]_0 = \frac{Y\,k_{d1}}{1-Y} + [L]_0\,Y + \frac{[I]_0\,Y\,k_{d1}}{k_{d2}\,(1-Y) + Y\,k_{d1}}$$

where $[L]_0$ and $[I]_0$ are the initial concentrations of Ac-(ATTO 655)KDADA and the unlabeled peptide, I, respectively, and Y, k_{d1} and k_{d2} are defined in Equations (4), (3) and (5), respectively. The Y versus [V] plot for Ac-(ATTO 655)KDADA in the presence of Ac_2KDADL (5 mM) is shown in Figure 2, and the k_d value in neat water for Ac_2KDADL was determined to be 260(±6) μM. The competitive binding assay was also used to determine the Van-binding affinity of Ac_2KDADA, which was found to be similar to that of Ac(ATTO 655)KDADA (Figure S2 in the Supporting Information); this suggests that the appended fluorophore does not affect the binding equilibrium. We note that the Van-binding affinity of the peptide ligand increased in the order of -D-Ala-D-Lac < -D-Ala-D-Ala. The loss of a hydrogen bond and a concomitant gain of an oxygen–oxygen lone pair repulsion between Ac_2KDADL and Van are, in part, responsible for the significant reduction in the degree of binding between the two moieties when compared to the peptide terminating in -D-Ala-D-Ala (Figure 3).[3,21]

The effects of buffers on the binding between Van and the various peptides are discussed next. When the solvent was changed from neat water to phosphate buffer (10 mM; consisting of 6.8 mM HPO_4^{2-} and 3.2 mM $H_2PO_4^-$, pH 7.3, ionic strength $\mu = 24$ mM) the Van-binding affinity of Ac-(ATTO 655)KDADA (i.e., $k_d = 1.3$ μM) did not vary significantly from the one observed in neat water, and the k_d determined by FCS was in agreement with previously reported values in phosphate buffers.[5] This suggests that the high affinity of Ac(ATTO 655)KDADA to Van is not influenced by the phosphate buffer. Figure 2 shows the Y versus [V] plots of Ac(ATTO 655)KDADA in the presence of Ac_2KDADL (5 mM) in phosphate buffer (5 mM; consisting 3.4 mM HPO_4^{2-} and 1.6 mM $H_2PO_4^-$, pH 7.3, $\mu = 12$ mM) and phosphate buffer (10 mM). It was observed that as the concentration of phosphate ions increases, a smaller initial concentration of Van is needed to achieve a large (relative) proportion of Ac(ATTO 655)KDADA–Van complex (i.e., Y). This means that the binding strength between Van and Ac_2KDADL significantly decreases when the phosphate buffer concentration is increased from 0 to 10 mM. The k_d value of Ac_2KDADL, obtained from Figure 2, increased

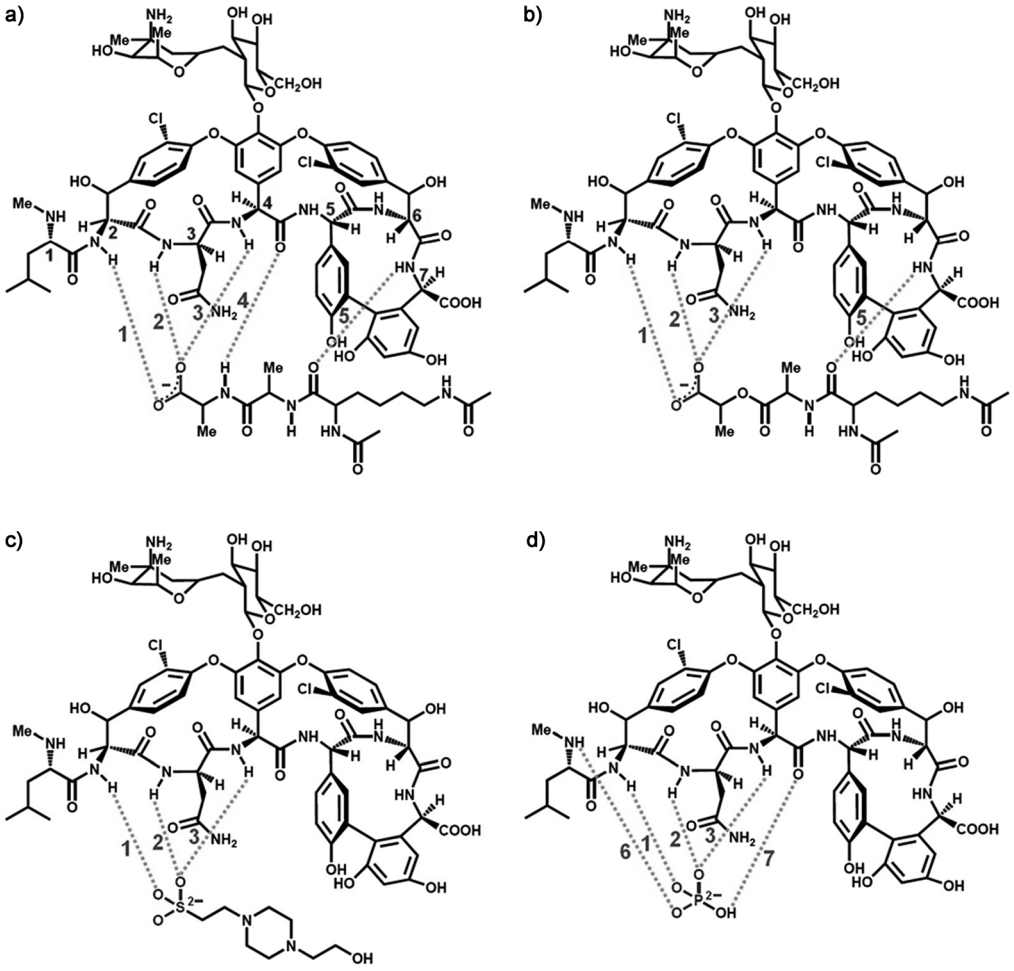

Figure 3. The binding interaction between the glycopeptide antibiotic vancomycin and: a) Ac_2KDADA, b) Ac_2KDADL, c) HEPES, and d) HPO_4^{2-}. Hydrogen bonds are indicated by dotted lines.

from 260 μM in neat water to 1040(±20) and 2140(±40) μM in 5 and 10 mM phosphate buffers, respectively. When the phosphate ion concentration was further increased by utilizing 20 mM phosphate buffer (consisting of 13.7 mM HPO_4^{2-}, 6.3 mM $H_2PO_4^-$, pH 7.3, $\mu = 47$ mM) the stability of the Ac_2KDADL–Van complex yielded a k_d (=1850(±50) μM) value close to that measured in 10 mM phosphate buffer. It is worth noting that the k_d values, determined by FCS, for the 10 and 20 mM phosphate buffers fall in the range previously reported for Ac_2KDADL in phosphate buffers (i.e., ca. 1800 to 3000 μM for buffer concentrations of 20 mM to 0.2 M).[5,8,13]

Similar behavior was also observed when the FCS measurements were conducted in HEPES buffer. In this case, $k_d = 1.1(\pm 0.1)$ μM was obtained for Ac(ATTO 655)KDADA in HEPES (10 mM), NaCl (6 mM) buffer (pH 7.3, $\mu =$ 10 mM). Perkins and Nieto have shown that the stability of the Ac_2KDADA–Van complex remains relatively unchanged in the pH range from 3 to 8 and at low ionic strengths as employed in this study.[12] Our results, therefore, suggest that the binding of the peptide terminating in D-Ala-D-Ala to Van is not affected by the buffer solution due to its high binding affinity. On the other hand, the association between Ac_2KDADL and Van is weakened as the concentration of HEPES increases (Figure 4). From the ligand competitive assay, k_d values for Ac_2KDADL in 5 mM HEPES, 6 mM NaCl buffer (pH 7.3, $\mu = 8$ mM) and 10 mM HEPES, 6 mM NaCl buffer were determined to be 677(±17) and 2870(±189) μM, respectively. We noted an approximately 8- to 11-times enhancement in k_d value on going from neat water to 10 mM phosphate or 10 mM HEPES, 6 mM NaCl buffer solutions; this further confirms that the components constituting the buffers (i.e., phosphate ions and HEPES) affect the molecular interaction between Van subunits and bacterial cell wall peptide analogues.

To determine if ionic strength plays a role in changing the Van-binding constant of Ac_2KDADL in phosphate buffer, the binding of Ac_2KDADL to Van in phosphate (5 mM), NaCl (12 mM) buffer (pH 7.3, $\mu = 24$ mM) was determined by using FCS and a k_d value of 1170(±70) μM was obtained, which is close to the k_d value measured in 5 mM phosphate buffer (i.e., in the absence of NaCl). Similarly, the k_d (= 3000(±80) μM) value determined from the FCS experiment in 10 mM HEPES buffer (pH 7.3, $\mu = 4$ mM) was close to that obtained in the 10 mM HEPES, 6 mM NaCl buffer. Therefore, ionic strengths used in this study do not significantly alter the binding/dissociation constant. The values of k_d and the corresponding change in free energy of binding ($\Delta G = -RT\ln k_d^{-1}$) for the peptides in different solvents are presented in Table 1.

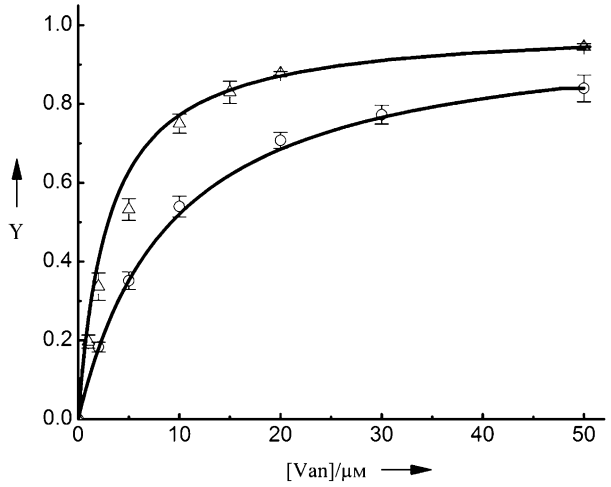

Figure 4. Plots of Y versus [Van] for Ac(ATTO 655)KDADA in the presence of Ac_2KDADL (5 mM) in 5 mM HEPES, 6 mM NaCl buffer (○) and 10 mM HEPES, 6 mM NaCl buffer (△).

Table 1. FCS determined k_d and ΔG for interactions between Van and Ac(ATTO 655)KDADA and Ac_2KDADL.

Ligand	Solvent	k_d [μM]	ΔG[a] [kcal mol^{-1}]
Ac(ATTO 655)KDADA	neat water	1.1±0.1	−8.1
	10 mM phosphate buffer	1.3±0.1	−8.0
	10 mM HEPES, 6 mM NaCl	1.1±0.1	−8.1
Ac_2KDADL	neat water	260±6	−4.9
	5 mM phosphate buffer	1040±20	−4.0
	10 mM phosphate buffer	2140±40	−3.6
	5 mM HEPES, 6 mM NaCl	677±17	−4.3
	10 mM HEPES, 6 mM NaCl	2870±189	−3.4

[a] $\Delta G = -RT\ln k_d^{-1}$.

To further assess the stability of the complexes formed between Van and the various affinity ligands (i.e., peptide precursors Ac_2KDADA and Ac_2KDADL, buffer ions $H_2PO_4^-$ and HPO_4^{2-}, and HEPES), MD simulation in an explicit water environment was performed. The final snapshots of the 10 ns MD simulations of the Van binding complexes are given in Figure 5. The corresponding values of the MD computed change in free energy of binding ΔG_{md} are given in Table S1 (in the Supporting Information). The qualitative trend in ΔG_{md} indicates a distribution of hydrogen bonding strengths in the binding complexes of Van with Ac_2KDADA, Ac_2KDADL, $H_2PO_4^-$, HPO_4^{2-}, and HEPES. According to the MD simulation, the carboxylate head-groups of Ac_2KDADA and Ac_2KDADL, sulfate group of HEPES, and phosphate group of HPO_4^{2-} are oriented toward the Van carboxylate binding site such that a minimal set of hydrogen bonding exists between the peptide/ligand and the antibiotic amide NH groups found in residues 2, 3, and 4 (hydrogen bonds labeled 1, 2 and 3 in Figure 3). We note that the value of ΔG_{md} is reduced from −14.7 to −6.0 kcal mol^{-1} on going from Ac_2KDADA to Ac_2KDADL. This is due to the missing central hydrogen bond (labeled 4 in Figure 3a) when the NH is substituted for an O in Ac_2KDADL; this results in the weakening of the hydrogen bond between the peptide and

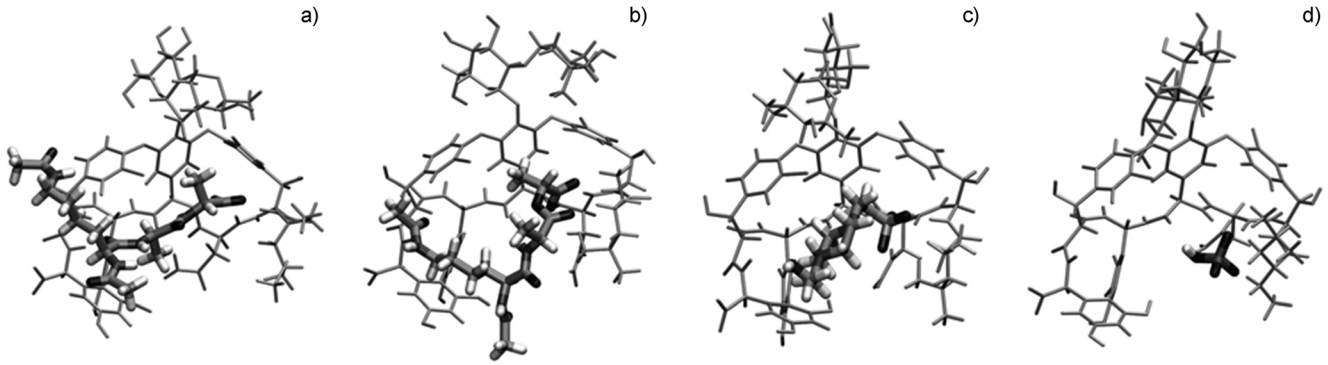

Figure 5. The final snapshot of the 10 ns MD simulation of vancomycin binding complex with: a) Ac_2KDADA, b) Ac_2KDADL, c) HEPES, and d) HPO_4^{2-}.

the amide NH found in both residue 4 (hydrogen bond labeled 3 in Figure 3b) and residue 7 (hydrogen bond labeled 5 in Figure 3b).

The MD simulation also reveals that the binding of Van to the hydrogen phosphate ion HPO_4^{2-} ($\Delta G_{md} = -7.4$ kcal mol^{-1}) appears to be slightly stronger than the binding to Ac_2KDADL but much weaker than the association between Ac_2KDADA and Van. Apart from hydrogen bonding with the amide NH groups of residues 2, 3, and 4 of Van, the complex formed between HPO_4^{2-} and Van is further stabilized by additional hydrogen bonds involving the amide NH group in residue 1 and the carbonyl group in residue 4 (hydrogen bonds labeled 6 and 7 in Figure 3d). On the other hand, dihydrogen phosphate ion $H_2PO_4^-$ appears to be bound only very weakly to the binding pocket of the antibiotic. Figure 6 shows the root-mean-square deviation (RMSD) fluctuations of the ligands and Van against the simulation time. It can be seen clearly that RMSD of $H_2PO_4^-$ fluctuates dramatically and leaves the original binding site at around 9 ns of simulation; this indicates that $H_2PO_4^-$ cannot be stabilized within the carboxylate binding site of Van. However, HPO_4^{2-} remained stable within the binding pocket of Van, even for simulation times of up to 50 ns (data not shown). Both Ac_2KDADL and HEPES undergo complexation with Van by means of three hydrogen bonds, however, the flexible framework of HEPES molecule under the influence of solvent molecules impairs its Van-binding affinity and leads to a lower free energy of binding ΔG_{md} (-3.1 kcal mol^{-1}).

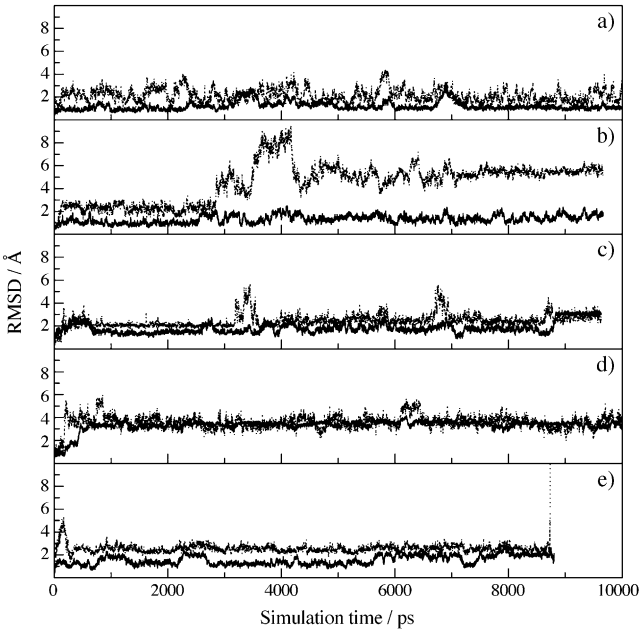

Figure 6. Root-mean-square deviations RMSD (Å) of: a) Ac_2KDADA, b) Ac_2KDADL, c) HEPES, d) HPO_4^{2-}, e) $H_2PO_4^-$ (dashed lines) with Van (solid lines) for 10 ns MD simulations.

In our FCS measurement, the reduction in the binding strength between Van and Ac_2KDADL, resulting from a change of solvent from neat water to buffer solution, might arise from effects associated with the HPO_4^{2-}–Van and HEPES–Van interaction. Aoki et al. have reported the crystal structures of complexes formed between Van and peptides terminating with the sequence -D-Ala-D-Lac and have shown that hydrogen bonding interaction between phosphate ions and Van is non-negligible.[22] In neat water, Ac_2KDADL is able to replace solvent water found in the antibiotic binding pocket after both desolvation and conformational rearrangement of the binding site have taken place.[23] On the other hand, expulsion of HPO_4^{2-} and HEPES from the binding pocket is relatively more difficult due to their stronger interactions with Van. Based on recent crystal structure studies,[22,24] a simple model is proposed whereby a water-mediated hydrogen bond interaction between the amide nitrogen of the Lys residue in Ac_2KDADL and the oxygen of the terminal carboxylate group of Van is necessary to achieve favorable peptide orientation and energy to remove and replace HPO_4^{2-} and HEPES from the binding site. This results in a loose Ac_2KDADL–Van complex in buffer solution as compared to neat water. On average, the number of Ac_2KDADL–Van complex decreases while the number of water, HPO_4^{2-} and HEPES filled Van available for binding to Ac(ATTO 655)KDADA increases as the buffer concentration is raised until an equilibrium point is reached. Ac_2KDADA binds strongly to Van and can, therefore, easily replace HPO_4^{2-} and HEPES from the binding pocket without significant variation in the stability of the

complex formed. Other considerations, such as cooperativity,[25] between the various factors influencing binding in the presence of HPO_4^{2-} and HEPES might be important but the exact nature of their roles is not clear at the present moment.

Conclusion

We have presented a systematic study to investigate the molecular interactions of glycopetide antibiotic vancomycin with different affinity ligands including Van-sensitive and Van-resistant bacterial cell wall peptide analogues and buffer ions by using both competitive FCS measurements and MD simulation. The FCS measurement clearly indicates a higher Van-binding affinity for the drug-sensitive bacteria cell wall precursor, Ac_2KDADA, as compared to the drug-resistant bacterial cell wall peptide analogue, Ac_2KDADL. The competitive FCS and MD simulation studies also demonstrate the profound effects of phosphate and HEPES buffers on the stability of the complexes formed between Van and the low-affinity Ac_2KDADL. The weak association between the buffer components and the binding pocket of Van has several important implications. In particular, the effects of phosphate and HEPES buffers on the binding between Van and antibiotic-resistant peptide analogues are significant and should not be ignored. Furthermore, there might exist components in the Van-resistant bacterial cell wall and its surrounding environment that are capable of binding to the antibiotic molecules leading to a perturbation and possible reduction in the drug's ability to directly associate and kill bacteria. Therefore, the design of Van derivatives that bind specifically to the termini D-Ala-D-Lac of the peptidoglycan without interference from surrounding chemical or biological species is a promising step towards increasing the efficacy of antibiotic drugs against bacterial pathogens and obtaining a more thorough understanding of the actual host–guest reaction mechanism of antibiotics.[26]

Experimental Section

Materials: Chemical reagents and solvents were used as received from Sigma–Aldrich unless otherwise stated. ATTO 655 NHS-ester, peptide precursors AcK(Ac)DADA and AcK(Ac)DADL and HEPES buffer (1 M) solution (pH 7.5) were purchased from ATTO-TECH GmbH (Germany), Bachem (Germany) and 1st BASE (Singapore). Vancomycin (Van, Sigma–Aldrich) was purified by using reversed-phase high performance liquid chromatography (RP-HPLC, Shimadzu). For analytical RP-HPLC, the measurement was conducted with an Alltima C-18 column (250 × 3.0 mm) at a flow rate of 1.0 mL min^{-1}, and semipreparative RP-HPLC was performed on a C-18 column (250 × 10 mm) at a flow rate of 3 mL min^{-1}. Absorption and fluorescence spectra were recorded by using a 5 mm path quartz cell on a Beckman Coulter DU800 spectrometer and a Cary Eclipse (Varian) fluorescence spectrometer, respectively. Millipore-purified (Milli-Q) water was used in all experiments.

Preparation of peptide ligand samples: The peptide precursors (including AcK(NH_2)DADA and AcK(NH_2)DADL) were synthesized by solid-phase peptide synthesis by using standard Fmoc chemistry. Briefly, 2-chlorotrityl chloride resin (200 mg, 1.0–1.5 mmol g^{-1} loading level) was placed into a reaction vessel of a peptide synthesizer and washed with DCM three times. The first amino acid was coupled to the resin under DIPEA (174.2 μL, 1 mmol) in DCM, and shaken for 30 min. After being washed with MeOH and DMF, deprotection of Fmoc was conducted with piperidine (20%) in DMF. The resin was then washed with DMF three times and subsequently subjected to the following series of coupling–deprotection cycles: i) coupling with amino acid (0.4 mmol), HOBT (108.1 mg, 0.8 mol), TBTU (256 mg, 0.8 mmol) and DIPEA (139.3 μL, 0.8 mmol), and shaken for 2 h, and ii) Fmoc deprotection was carried out as stated above following three times DMF wash. After three cycles, the peptide sequence was coupled with acetic anhydride (1.2 mL, 30% v/v), DIPEA (1 mL, 50% v/v) and DMF (0.4 mL, 20% v/v) and shaken, overnight. The product was cleaved from the solid support by treatment with TFA/triisopropylsilane/anisole (2:1:1) and collected as white solids.

After obtaining the peptide ligands, ATTO 655 NHS-ester (1 mg, 1 μM) was labeled onto the peptides (1.4 mg, 4 μM) by treatment for 4 h in anhydrous DMF and TEA under nitrogen. The products were purified by RP-HPLC and characterized by using electrospray mass spectrometry. For the fluorescent-labeled peptides, the peaks at m/z 840.35 and 840.96 correspond to M^+ of Ac(ATTO 655)KDADA and Ac-(ATTO 655)KDADL, respectively (Figure S1 in the Supporting Information).

For the FCS measurements, the non-labeled peptide precursors, ATTO 655-labeled peptide ligands and vancomycin were dissolved in different solvents (neat water, phosphate buffer and HEPES buffer) to obtain the stock solutions. The concentration of the stock solution of ATTO 655-labeled peptide ligand was determined by using the Beer–Lambert law. Solutions used in the FCS experiments were freshly prepared from stock solutions by serial dilution. For the FCS assay, the samples were prepared by mixing the dye-labeled peptide and Van in neat water, phosphate buffer or HEPES buffer. In the case of the FCS competitive binding assay, the dye-labeled peptide, Van and Ac_2KDADA/Ac_2KDADL were sequentially added into either neat water or buffer solutions. In all measurements, the final concentrations of dye-labeled peptide ligand and Ac_2KDADA/Ac_2KDADL were 1.5 nM and 5 μM/5 mM, respectively, and the concentration of Van was between 0 and 50 μM.

Fluorescence correlation spectroscopy (FCS): FCS measurements were performed by using a time-resolved confocal microscope (MicroTime 200, PicoQuant). The excitation source used was a 635 nm pulsed diode laser (LDH-P-C-635B, PicoQuant) with a repetition rate of 20 MHz. The excitation light passed through an excitation filter (Z636/10, Chroma) and directed via a dichroic mirror (Z638rpc, Chroma) into an inverted microscope (IX71, Olympus) before being focused onto the sample through a water objective lens (60×, N.A. 1.2, Olympus). The correction collar of the water immersion objective was optimized in order to obtain the highest signal-to-noise ratio and the fluorescence was subsequently collected by the same objective lens. The fluorescence was then passed through the dichroic mirror, an emission filter (HQ685/70, Chroma) and refocused through a pinhole (50 μm in diameter) before being detected by an avalanche photodiode (SPCM-AQR-15, Perkin–Elmer). The excitation intensity of the laser beam used was 5.8 kW cm^{-2}.

The lateral radius (ω_0) and axial $1/e^2$ radius (z_0) of the confocal volume were determined by measuring the autocorrelation function of ATTO 655-COOH in water. Assuming that the confocal volume can be approximated by a three-dimensional Gaussian function, ω_0 and z_0 were obtained by fitting the autocorrelation function ($G(t)$) of ATTO 655-COOH in water by using Equation (1) and then by applying Equation (2). The diffusion coefficient of ATTO 655-COOH in water at 23 °C was previously reported to be $D = 404\ \mu m^2 s^{-1}$.[18] The number of fluorescent molecules (N) was obtained from $G(t)$ when $t = 0$ (i.e., $N = G_0^{-1}$).

The binding constant of Ac(ATTO 655)KDADA was determined by measuring the FCS autocorrelation functions of the dye-labeled peptide ligand in varying amounts of Van. Basically, a dilute solution of Ac-(ATTO 655)KDADA in either neat water or buffer solutions (concentration of 1.5 nM) was incubated with an appropriate amount of Van (between 0 to 50 μM) at ambient conditions before the FCS measurements were conducted. The binding constants between Van and the unlabeled Ac_2KDADA and Ac_2KDADL peptides were determined by using competi-

tive binding. In this case, Van was added to a mixture containing Ac-(ATTO 655)KDADA (1.5 nM) and Ac_2KDADL (5 mM) or Ac_2KDADA (5 μM). All the FCS measurements were repeated at least three times for each Van concentration and the results were averaged.

Molecular dynamics (MD) simulations: Each molecule was first optimized at the AM1 level by using the Gaussian 03 package and the minimized structure was used to calculate the B3LYP/6-31G* electrostatic potential (ESP). The atomic charges used for molecular mechanics calculations were derived from the ESP by using the RESP program implemented in the AMBER 9.0 package.

For the ligands (Ac_2KDADA, Ac_2KDADL, HEPES, HPO_4^{2-} and $H_2PO_4^-$) studied here, the binding orientations were first estimated by using AutoDock 4.0. The preliminary docking study showed that the vancomycin carboxylate binding site is the site for docking to either sulfate or phosphate. We thus used this site to generate the receptor site and the energetic grids for the docking calculations. Flexible docking was performed in which single bonds outside the rings were set free to rotate. During the docking process, conformational search was performed by using the Solis and Wets local search method, and the Lamarckian genetic algorithm was applied to find minimum energy structure of the ligand–receptor complexes.

The docking structures obtained were then minimized by using 1000 steps of Steepest Descent followed by another 3000 steps of Conjugate Gradient. Molecular dynamics simulations were carried out by using the SANDER module of the AMBER 9.0 program. For each binding complex obtained from AutoDock, about 2000 TIP3P water molecules with 10 Å buffer were added around the complex. K^+ counterions were added to maintain the neutrality of the system. The simulations were carried out at 300 K with a time step of 1.0 fs. The non-bonded cutoff was set to 10.0 Å and SHAKE algorithm was applied for all the bonds involving hydrogen atoms. After minimization of 4000 steps and equilibration for 100 ps, complex conformations were collected every 0.5 ps for the following 10 ns simulation. Finally, 1000 snapshots were collected from the region with stable fluctuation for post-processing analysis and free energy calculations.

For each snapshot collected during the MD simulation, both interaction energies (ΔE_{vdw}, ΔE_{elec}) and the electrostatic contribution ($\Delta\Delta G_{PB}$) to the solvation energy were calculated with the PBSA program of AMBER 9.0. The non-polar part of the solvation energy ($\Delta\Delta G_{SA}$) was estimated by using the simple empirical relation: $\Delta\Delta G_{SA} = cA + b$, where A is the solvent-accessible surface area that is estimated with Sanner's algorithm implemented in the MSMS program with a solvent probe radius of 1.4 Å and the PARSE atomic radii parameters; and c and b are empirical constants and were set to 0.00542 and 0.92 kcal mol^{-1}, respectively. The energy terms obtained with the MM-PBSA approach were then averaged over 100 time frames. The normal mode calculation to estimate the entropy contribution was performed by using Nmode module in the AMBER 9.0 program (Tables S1 and S2 in the Supporting Information).

Acknowledgements

The authors gratefully acknowledge NTU Start-Up grant (SUG), Tier 1 RG64/10 and A*Star BMRC grant 07/1/22/19/534.

[1] a) J. C. J. Barna, D. H. Williams, *Annu. Rev. Microbiol.* **1984**, *38*, 339–345; b) L. H. Li, B. Xu, *Curr. Pharm. Des.* **2005**, *11*, 3111–3124; c) D. Kahne, C. Leimkuhler, W. Lu, C. Walsh, *Chem. Rev.* **2005**, *105*, 425–448.

[2] a) K. Koteva, H. Hong, X. D. Wang, I. Nazi, D. Hughes, M. J. Naldrett, M. J. Buttner, G. D. Wright, *Nat. Chem. Biol.* **2010**, *6*, 327–329; b) M. Nieto, H. R. Perkins, *Biochem. J.* **1971**, *123*, 773–787; c) B. G. Xing, C. W. Yu, P. L. Ho, K. H. Chow, T. Cheung, H. W. Gu, Z. W. Cai, B. Xu, *J. Med. Chem.* **2003**, *46*, 4904–4909; d) B. G. Xing, P. L. Ho, C. W. Yu, K. H. Chow, H. W. Gu, B. Xu, *Chem. Commun.* **2003**, 2224–2225; e) B. G. Xing, T. T. Jiang, W. G. Bi, Y. M. Yang, L. H. Li, M. L. Ma, C. K. Chang, B. Xu, E. K. L. Yeow, *Chem. Commun.* **2011**, *47*, 1601–1603; f) B. G. Xing, C. W. Yu, K. H. Chow, P. L. Ho, D. G. Fu, B. Xu, *J. Am. Chem. Soc.* **2002**, *124*, 14846–14847.

[3] C. C. McComas, B. M. Crowley, D. L. Boger, *J. Am. Chem. Soc.* **2003**, *125*, 9314–9315.

[4] M. P. Williamson, D. H. Williams, S. J. Hammond, *Tetrahedron* **1984**, *40*, 569–577.

[5] P. H. Popieniek, R. F. Pratt, *Anal. Biochem.* **1987**, *165*, 108–113.

[6] P. H. Popieniek, R. F. Pratt, *J. Am. Chem. Soc.* **1991**, *113*, 2264–2270.

[7] U. N. Sundram, J. H. Griffin, T. I. Nicas, *J. Am. Chem. Soc.* **1996**, *118*, 13107–13108.

[8] a) N. E. Allen, D. L. LeTourneau, J. N. Hobbs, Jr., *J. Antibiot.* **1997**, *50*, 677–684; b) N. E. Allen, D. L. LeTourneau, J. N. Hobbs, Jr., *Antimicrob. Agents Chemother.* **1997**, *41*, 66–71.

[9] J. Rao, I. J. Colton, G. M. Whitesides, *J. Am. Chem. Soc.* **1997**, *119*, 9336–9340.

[10] a) D. H. Williams, J. P. L. Cox, A. J. Doig, M. Gardner, U. Gerhard, P. T. Kaye, A. R. Lal, I. A. Nicholls, C. J. Salter, R. C. Mitchell, *J. Am. Chem. Soc.* **1991**, *113*, 7020–7030; b) M. S. Searle, D. H. Williams, U. Gerhard, *J. Am. Chem. Soc.* **1992**, *114*, 10697–10704.

[11] a) Z. Yang, E. R. Vorpagel, J. Laskin, *J. Am. Chem. Soc.* **2008**, *130*, 13013–13022; b) Z. Yang, E. R. Vorpagel, J. Laskin, *Chem. Eur. J.* **2009**, *15*, 2081–2090.

[12] H. R. Perkins, M. Nieto, *Ann. N. Y. Acad. Sci.* **1974**, *235*, 348–363.

[13] J. Rao, L. Yan, J. Lahiri, G. M. Whitesides, R. M. Weis, H. S. Warren, *Chem. Biol.* **1999**, *6*, 353–359.

[14] P. J. Vollmerhaus, F. W. A. Tempels, J. J. Kettenes-van den Bosch, A. J. R. Heck, *Electrophoresis* **2002**, *23*, 868–879.

[15] G. A. Grant, X. L. Xu, Z. Hu, A. R. Purvis, *Biochemistry* **1999**, *38*, 16548–16552.

[16] J. P. Schuermann, M. T. Henzl, S. L. Deutscher, J. T. Tanner, *Proteins Struct. Funct. Bioinf.* **2004**, *57*, 269–278.

[17] a) S. T. Hess, S. Huang, A. A. Heikal, W. W. Webb, *Biochemistry* **2002**, *41*, 697–705; b) E. Haustein, P. Schwille, *Methods* **2003**, *29*, 153–166; c) X. Chen, Y. Zhou, P. Qu, X. S. Zhao, *J. Am. Chem. Soc.* **2008**, *130*, 16947–16952.

[18] a) T. Dertinger, V. Pacheco, I. von der Hocht, R. Hartmann, I. Gregor, J. Enderlein, *ChemPhysChem* **2007**, *8*, 433–443; b) C. B. Müller, A. Loman, V. Pacheco, F. Koberling, D. Willbold, W. Richtering, J. Enderlein, *Europhys. Lett.* **2008**, *83*, 46001; c) V. Buschmann, B. Krämer, F. Koberling, R. Macdonald, S. Rüttinger, *PicoQuant Application Note, Quantitative FCS: Determination of the confocal volume by FCS and bead scanning with MicroTime 200*.

[19] J. Schüler, J. Frank, U. Trier, M. Schäfer-Korting, W. Saenger, *Biochemistry* **1999**, *38*, 8402–8408.

[20] Z.-X. Wang, *FEBS Lett.* **1995**, *360*, 111–114.

[21] J.-G. Lee, C. Sagui, C. Roland, *J. Am. Chem. Soc.* **2004**, *126*, 8384–8385.

[22] T. Kikuchi, S. Karki, I. Fujisawa, Y. Matsushima, Y. Nitanai, K. Aoki, *Bull. Chem. Soc. Jpn.* **2010**, *83*, 391–400.

[23] S. Jusuf, P. H. Axelsen, *Biochemistry* **2004**, *43*, 15446–15452.

[24] Y. Nitanai, T. Kikuchi, K. Kakoi, S. Hanamaki, I. Fujisawa, K. Aoki, *J. Mol. Biol.* **2009**, *385*, 1422–1432.

[25] a) D. H. Williams, M. S. Westwell, *Chem. Soc. Rev.* **1998**, *27*, 57–63; b) D. H. Williams, E. Stephens, D. P. O'Brien, M. Zhou, *Angew. Chem.* **2004**, *116*, 6760–6782; *Angew. Chem. Int. Ed.* **2004**, *43*, 6596–6616.

[26] J. F. Fisher, S. Mobashery, *J. Med. Chem.* **2010**, *53*, 4813–4829.

Received: July 18, 2011
Published online: November 14, 2011

